Ichiro Yamada, MD
Winn Aung, MD
Yoshiro Himeno, MD
Tsuneaki Nakagawa, MD
Hitoshi Shibuya, MD

Index terms:
Liver neoplasms, diagnosis, 761.312, 761.3194, 761.32, 761.33
Liver neoplasms, MR, 761.121411, 761.121416, 761.12144
Magnetic resonance (MR), diffusion study, 761.12144
Magnetic resonance (MR), echo planar, 761.121416
Magnetic resonance (MR), technology, 761.121416

Radiology 1999; 210:617–623

Abbreviations:
ADC = apparent diffusion coefficient
IVIM = intravoxel incoherent motion
MPG = motion-probing gradient

[1] From the Department of Radiology, Faculty of Medicine, Tokyo Medical and Dental University, 1-5-45 Yushima, Bunkyo-ku, Tokyo 113-8519, Japan. Received March 16, 1998; revision requested May 22; revision received June 24; accepted August 10. **Address reprint requests to** I.Y.

Author contributions:
Guarantor of integrity of entire study, I.Y.; study concepts and design, I.Y., W.A.; definition of intellectual content, I.Y., W.A.; literature research, I.Y., Y.H.; clinical studies, I.Y., Y.H.; data acquisition, I.Y., T.N.; data analysis, I.Y., W.A.; statistical analysis, I.Y., T.N.; manuscript preparation, I.Y., W.A.; manuscript editing, I.Y.; manuscript review, I.Y., H.S.

Diffusion Coefficients in Abdominal Organs and Hepatic Lesions: Evaluation with Intravoxel Incoherent Motion Echo-planar MR Imaging[1]

PURPOSE: To determine the true diffusion coefficients of abdominal organs and hepatic lesions with intravoxel incoherent motion (IVIM) echo-planar magnetic resonance (MR) imaging.

MATERIALS AND METHODS: Seventy-eight patients suspected of having hepatic lesions were examined with IVIM echo-planar MR imaging at 1.5 T. There were 77 hepatic masses (27 hepatocellular carcinomas, 10 metastatic tumors, eight hemangiomas, and 32 cysts) in the 78 patients. The true diffusion coefficient *D* and the perfusion fraction *f* were calculated and compared with the apparent diffusion coefficient (ADC).

RESULTS: Specific values of *D* were found for abdominal organs (liver, 0.72×10^{-3} mm^2/sec; spleen, 0.80×10^{-3} mm^2/sec; kidney, 1.38×10^{-3} mm^2/sec; gallbladder, 2.82×10^{-3} mm^2/sec) and for hepatic lesions (hepatocellular carcinoma, 1.02×10^{-3} mm^2/sec; metastasis, 1.16×10^{-3} mm^2/sec; hemangioma, 1.31×10^{-3} mm^2/sec; cysts, 3.03×10^{-3} mm^2/sec). The ADCs of solid organs and solid lesions were significantly higher than their *D* values, indicating a high contribution of perfusion to the ADCs.

CONCLUSION: Perfusion contributes to the ADCs of abdominal organs and hepatic lesions. The *D* and *f* values are useful for the characterization of hepatic lesions.

The term intravoxel incoherent motion (IVIM) is used in reference to the microscopic translations that occur in voxels on magnetic resonance (MR) images (1). The small movements in biologic tissue include the molecular diffusion of water and the microcirculation of blood (perfusion). Molecular diffusion is determined by the physical properties that allow a tissue to be characterized. Because of the pseudorandom organization of the capillary network at the voxel level, the microcirculation of blood, or perfusion, can also be considered to be an incoherent motion. IVIMs are quantified by means of a parameter termed the apparent diffusion coefficient (ADC). The ADC incorporates the effects of both diffusion and perfusion (2,3) and is equal to the true diffusion coefficient *D* when diffusion is the only type of motion present. In in vivo tissues, however, the reported (1) ADCs have often had higher values than expected. These high values have been attributed to the microcirculation of blood in the capillaries.

Diffusion-weighted MR imaging has recently been used to characterize abdominal organs and hepatic lesions (4,5). However, there are considerable discrepancies in the ADC values in previous reports (4–7), and there is still controversy about accurate ADC values. We postulated that the discrepancies could be due to varying amounts of perfusion in the ADCs. The purpose of this study was to investigate how perfusion contributes to the ADC of abdominal organs and hepatic lesions and to determine the true diffusion coefficient *D* with IVIM echo-planar MR imaging.

MATERIALS AND METHODS

Patients

During 2 years (1997–1998), 78 consecutive patients (53 men, 25 women; age range 24–79 years; mean age, 62 years) who were suspected of having hepatic lesions were examined with IVIM echo-planar MR imaging. In addition, 31 of the patients had cirrhosis of the liver.

There were a total of 77 hepatic masses in the 78 patients. Thirty-seven masses were malignant tumors (27 hepatocellular carcinomas and 10 metastatic tumors). For all hepatocellular carcinomas, the diagnosis was confirmed with biopsy and/or surgical findings. Seven metastatic tumors were diagnosed with biopsy and/or surgical findings, and the remaining metastatic tumors showed lesion progression on serial computed tomographic (CT) scans. The diagnosis in eight hepatic masses was cavernous hemangioma, and the diagnosis in 32 masses was liver cyst on the basis of typical findings on contrast agent–enhanced CT scans. The diagnosis of hemangioma was established with the appearance of slightly irregular or nodular peripheral enhancement immediately after injection of a bolus of iohexol (Omnipaque 300; Daiichi Seiyaku, Tokyo, Japan) that gradually filled in toward the center on delayed images obtained at dynamic contrast-enhanced CT (5).

The study protocol was approved by the institutional review board, and informed consent was obtained from all patients.

TABLE 1
Diffusion Coefficients of Abdominal Organs in 78 Patients

Organ	Diffusion Coefficient *D* ($\times 10^{-3}$ mm²/sec)	Perfusion Fraction *f*	ADC ($\times 10^{-3}$ mm²/sec)
Liver			
Normal ($n = 47$)	0.76 ± 0.27	0.29 ± 0.14	0.87 ± 0.26*
Cirrhotic ($n = 31$)	0.67 ± 0.25	0.23 ± 0.18	0.84 ± 0.22*
Overall ($n = 78$)	0.72 ± 0.27	0.26 ± 0.13	0.86 ± 0.25*
Spleen ($n = 76$)	0.80 ± 0.33	0.31 ± 0.13	0.88 ± 0.33*
Kidney ($n = 78$)	1.38 ± 0.29	0.33 ± 0.18	1.55 ± 0.27*
Pancreas ($n = 78$)	0.76 ± 0.33	0.30 ± 0.15	1.02 ± 0.28*
Muscle ($n = 78$)	0.69 ± 0.28	0.23 ± 0.16	1.09 ± 0.31*
Gallbladder ($n = 62$)	2.82 ± 0.60	0.00 ± 0.01	2.81 ± 0.36
Ascites ($n = 5$)	3.06 ± 0.48	0.01 ± 0.01	3.04 ± 0.39

Note.—Numbers are the mean ± SD.
* The ADC value was significantly higher than the *D* value ($P < .01$).

TABLE 2
Diffusion Coefficients of Hepatic Lesions in 78 Patients

Lesion	Diffusion Coefficient *D* ($\times 10^{-3}$ mm²/sec)	Perfusion Fraction *f*	ADC ($\times 10^{-3}$ mm²/sec)
Hepatocellular carcinoma ($n = 27$)	1.02 ± 0.17	0.15 ± 0.07	1.10 ± 0.18*
Metastasis ($n = 10$)	1.16 ± 0.18	0.22 ± 0.09	1.26 ± 0.25*
Hemangioma ($n = 8$)	1.31 ± 0.21	0.35 ± 0.10	1.56 ± 0.22*
Cyst ($n = 32$)	3.03 ± 0.22	0.00 ± 0.01	3.01 ± 0.28

Note.—Numbers are the mean ± SD.
* The ADC value was significantly higher than the *D* value ($P < .05$).

Imaging Examinations

A 1.5-T superconducting MR system (Magnetom Vision; Siemens, Erlangen, Germany) with a 25 mT/m maximum gradient capability and a body phased-array coil was used to obtain all MR images. Initially, all patients underwent conventional MR imaging. A T1-weighted fast low-angle shot sequence (150/4.1 [repetition time msec/echo time msec]; flip angle, 80°) and a T2-weighted turbo spin-echo sequence (2,595/128 [repetition time msec/effective echo time msec]; echo train length, 23) were performed with a matrix of 224 × 256, a field of view of 260–340 mm, a section thickness of 8 mm with an intersection gap of 2 mm, and one signal acquired.

A diffusion-weighted multisection spin-echo type of echo-planar imaging sequence that combined the motion-probing gradients (MPGs) before and after the 180° pulse with an echo-planar imaging readout was used for IVIM echo-planar MR imaging. The sequence was repeated for four values of the MPG, yielding images with four diffusion weightings for each section. The effect of IVIM is to produce attenuation of the signal intensity in each pixel, which is given by the following equation:

$$SI/SI_o = \exp(-b \times ADC), \qquad (1)$$

where SI is the signal intensity in the pixel with the diffusion gradient, SI_o is the signal intensity in the pixel without diffusion gradient, and b is the gradient factor (in seconds per square millimeter) of the pulse sequence; ADC is expressed as square millimeters per second in the pixel. An echo time of 123 msec, a bandwidth of 1,250 Hz per pixel, and 128 lines of data acquired in 0.3 second were the parameters used for sequential sampling of the k space. The other imaging parameters included a field of view of 340 mm, a 128 × 128 matrix, a section thickness of 8 mm with an intersection gap of 2 mm, and one signal acquired.

Fat suppression was performed by placing the frequency-selective radio-frequency pulse before the pulse sequence. The sequence was modified by adding MPGs on both sides of the 180° pulse along the section-selective direction. The MPGs used in this study had a duration (δ) of 26 msec, a separation time (Δ) of 59.7 msec, and a gradient strength (G) of 3.5, 11.0, 19.1 or 21.1 mT/m. The resultant values for the gradient factor b were 30, 300, 900, or 1,100 sec/mm². All images were acquired during a period of breath holding, so that respiratory movement would be absent.

Image Analysis

Initially, the decrease in the signal intensity of the hepatic lesions was compared with the signal intensity of the spleen. On the basis of the IVIM theory (2,3), we estimated signal attenuation by using the following equation:

$$SI/SI_o = (1 - f) \times \exp(-bD) + f \times \exp(-bD^*), \qquad (2)$$

where D and D^* are the true diffusion coefficient and the pseudodiffusion coefficient, respectively, and f is the fractional volume occupied in the voxel by flowing spins (ie, perfusion fraction).

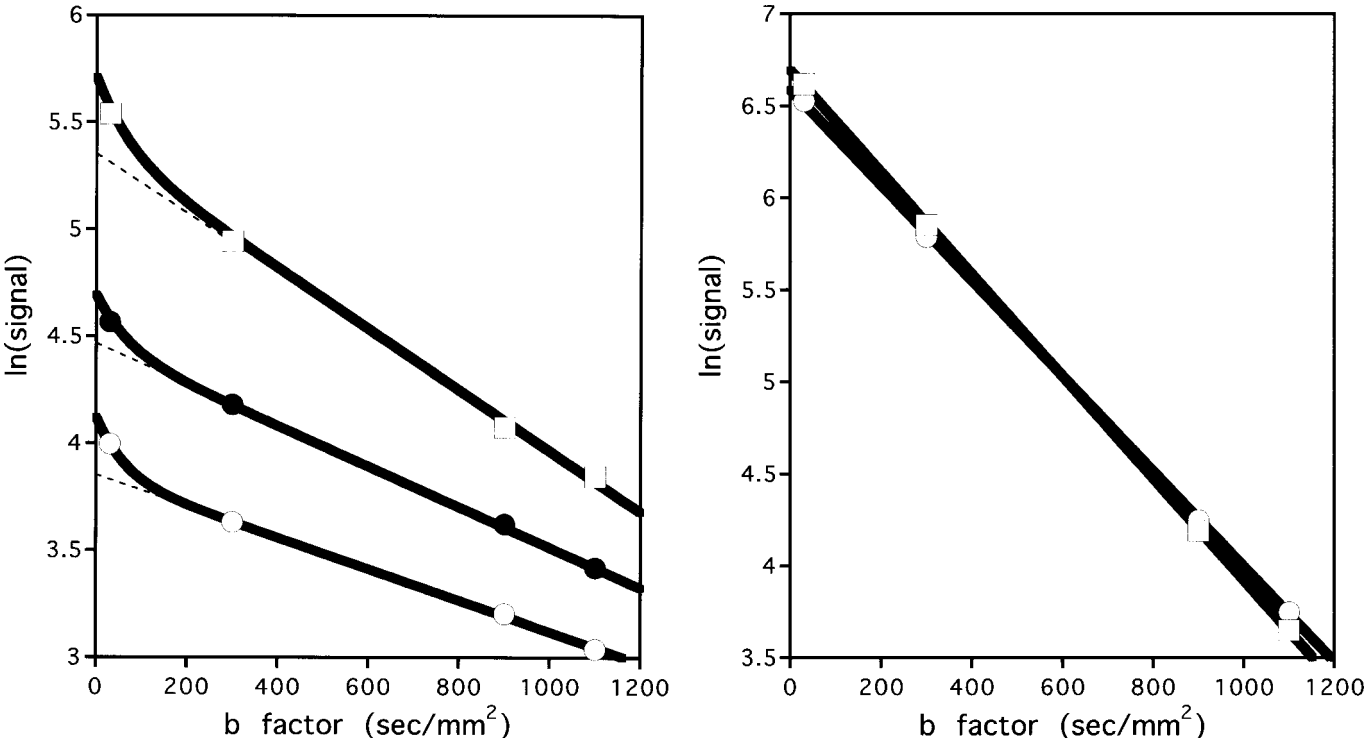

Figure 1. **(a)** Graph of signal attenuation versus *b* factor for the liver (○), kidney (□), and hepatocellular carcinoma (●) as measured at IVIM echo-planar MR imaging. The plots clearly show a curvature for low *b* values, which is indicative of perfusion effects, according to the IVIM theory. The dotted lines represent a least-squares fit to the last three data points. The slope of the straight line gives the diffusion coefficient *D*, and the deviation from the diffusion asymptote at the intercept gives the perfusion fraction *f* (2,3). **(b)** Graph of signal attenuation versus *b* factor for the gallbladder (○) and liver cysts (□) as measured at IVIM echo-planar MR imaging. The plots follow a straight line, as expected for a pure diffusion process. The slope of the straight line gives the diffusion coefficient *D*.

By using the Levenberg-Marquardt nonlinear least-squares algorithm, the signal intensities on four images obtained with different *b* factors were used in Equation (2), so that the *D*, *f*, and *D** values were calculated for the abdominal organs and hepatic lesions. The biexponential variation of the signal attenuation versus *b* was used to manifest the presence of incoherent motion other than diffusion (2,3). In the presence of perfusion, the signal attenuation is larger than that caused by diffusion alone, and the effect of perfusion is observed as a pseudodiffusion process (1–3). On the basis of Equation (1), the ADC value was calculated by using linear regression analysis with the natural logarithm of the signal intensity and the variable *b* from the four images (4).

Analysis was performed in regions of interest placed on different abdominal organs or hepatic lesions. All reported quantitative measurements of diffusion were made by means of an analysis of regions of interest. The regions of interest placed on the different organs consisted of at least 100 pixels. For abdominal organs, circular regions of interest were drawn in each organ, and the mean value of three or four regions of interest was calculated in each patient. For hepatic lesions, a circular region of interest was drawn to encompass as much of the lesion as possible. Diffusion coefficient maps were calculated on a pixel-by-pixel basis by using Equation (2). When there was a considerable misregistration of sections or when the lesions were very small, only the diffusion calculation was performed. This was the case in four (5%) of the 78 patients. The diffusion calculation was reliable, however, because it was based on the signal intensity on the original diffusion-weighted MR images.

An independent, blinded evaluation of the MR images was performed by two radiologists (I.Y., W.A.) who had no knowledge of the diagnosis of the hepatic lesions. When the observers could not agree, a diagnosis was achieved after discussion.

Statistical analysis was performed by using the Student *t* test for comparisons between groups. A one-way analysis of variance was used to test the diffusion values of the hepatic lesions. *P* values of less than .05 were considered to indicate statistically significant differences.

RESULTS

Diffusion-weighted images were obtained in all 78 patients, and diffusion coefficient maps could be obtained in 74 (95%). Chemical shift of the abdominal wall was observed in all patients. Because this artifact occurred in the same location, however, it did not preclude the measurement of diffusion coefficients in any patient. Furthermore, there were no cases of technical failure in this series.

Abdominal Organs

The values of *D*, *f*, and ADC for the liver, spleen, kidney, pancreas, muscle, gallbladder, and ascites were consistent for the patients and were specific for each organ (Table 1). The true diffusion coefficient *D* values were as follows: liver, 0.72×10^{-3} mm²/sec; spleen, 0.80×10^{-3} mm²/sec; kidney, 1.38×10^{-3} mm²/sec; pancreas, 0.76×10^{-3} mm²/sec; muscle,

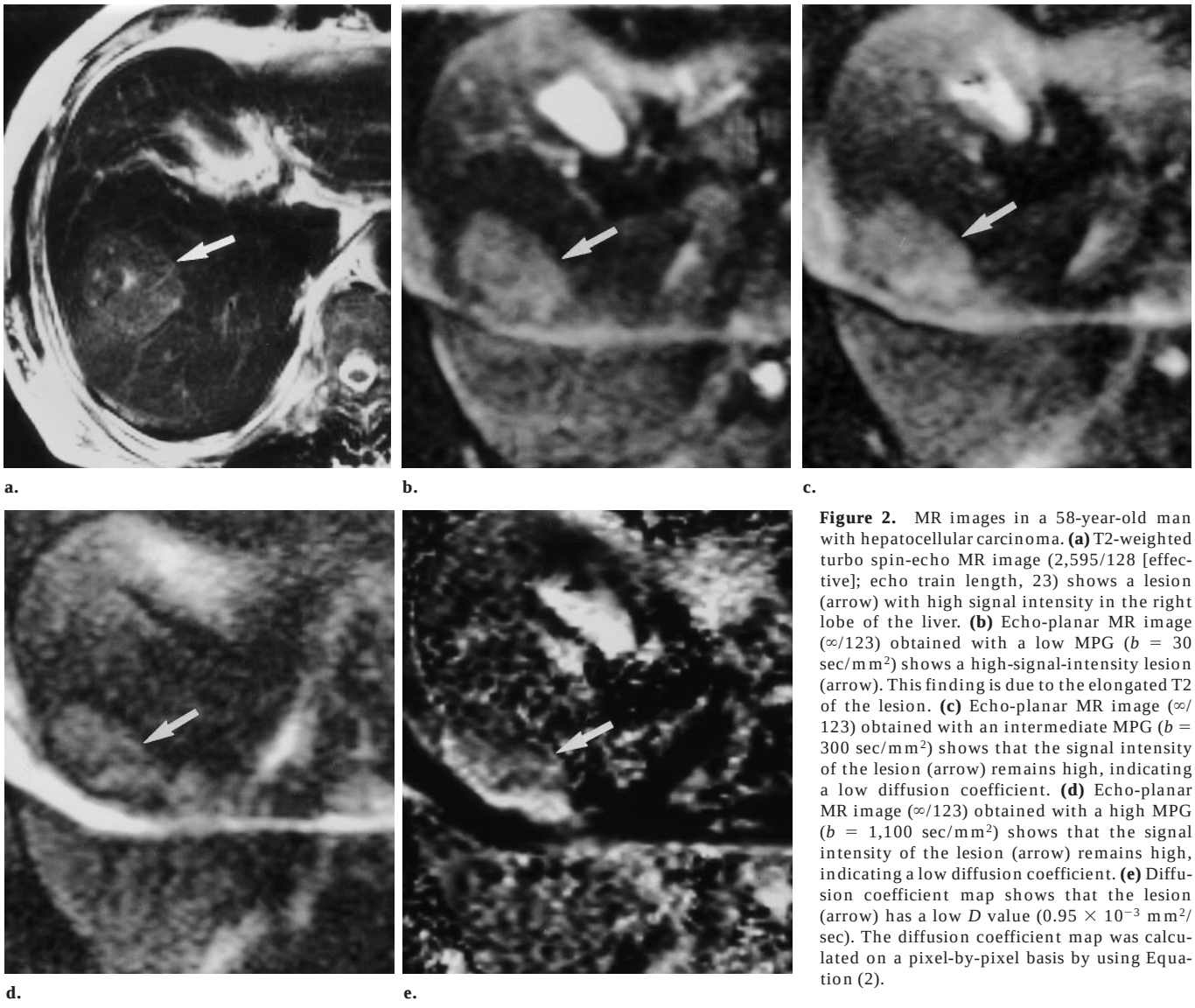

Figure 2. MR images in a 58-year-old man with hepatocellular carcinoma. **(a)** T2-weighted turbo spin-echo MR image (2,595/128 [effective]; echo train length, 23) shows a lesion (arrow) with high signal intensity in the right lobe of the liver. **(b)** Echo-planar MR image (∞/123) obtained with a low MPG (b = 30 sec/mm^2) shows a high-signal-intensity lesion (arrow). This finding is due to the elongated T2 of the lesion. **(c)** Echo-planar MR image (∞/123) obtained with an intermediate MPG (b = 300 sec/mm^2) shows that the signal intensity of the lesion (arrow) remains high, indicating a low diffusion coefficient. **(d)** Echo-planar MR image (∞/123) obtained with a high MPG (b = 1,100 sec/mm^2) shows that the signal intensity of the lesion (arrow) remains high, indicating a low diffusion coefficient. **(e)** Diffusion coefficient map shows that the lesion (arrow) has a low D value (0.95×10^{-3} mm^2/sec). The diffusion coefficient map was calculated on a pixel-by-pixel basis by using Equation (2).

0.69×10^{-3} mm^2/sec; gallbladder, 2.82×10^{-3} mm^2/sec; and ascites, 3.06×10^{-3} mm^2/sec (Fig 1). The D value for cirrhotic liver (0.67×10^{-3} mm^2/sec) was slightly lower than that for normal liver (0.76×10^{-3} mm^2/sec), but this difference was not statistically significant. The SDs shown in Table 1 represent the intersubject variability. We found no substantial degradation in the quality of diffusion-weighted MR images, and there was no substantial intrapatient variability for these measurements.

As shown in Table 1, the ADC values of the liver, spleen, kidney, pancreas, and muscle were significantly higher than the respective D values ($P < .01$) (Fig 1a). These results demonstrate that in diffusion-weighted IVIM MR imaging, the effect of perfusion indeed contributed to the ADC values of the abdominal solid organs. Moreover, the perfusion fractions of these organs were estimated to be as follows: liver, 0.26; spleen, 0.31; kidney, 0.33; pancreas, 0.30; and muscle, 0.23. The perfusion fraction for cirrhotic liver (0.23) was slightly lower than that for normal liver (0.29), but this difference was not statistically significant.

The ADC values of the gallbladder and ascites were, however, equal to or not significantly different from their respective D values (Table 1, Fig 1b). The ADC of a water phantom (2.27×10^{-3} mm^2/sec) also was equal to the D value (2.27×10^{-3} mm^2/sec). Furthermore, the perfusion fractions in these fluids were all confirmed to be 0 or nearly 0. These data are compatible with the fact that diffusion is the only type of motion in the gallbladder (bile), ascites fluid, and water phantom.

Hepatic Lesions

The values of the variables D, f, and ADC in the various hepatic lesions were different from those in normal liver (Table 2). The values of D were as follows: hepatocellular carcinomas, 1.02×10^{-3} mm^2/sec; metastases, 1.16×10^{-3} mm^2/sec; hemangiomas, 1.31×10^{-3} mm^2/sec; and cysts, 3.03×10^{-3} mm^2/sec (Figs 1–3). In our series, there were no cases of cystic metastases, and all of the metastatic lesions were solid tumors.

As shown in Table 2, the ADC values of hepatocellular carcinomas, metastases, and hemangiomas were significantly higher than the D values of these lesions

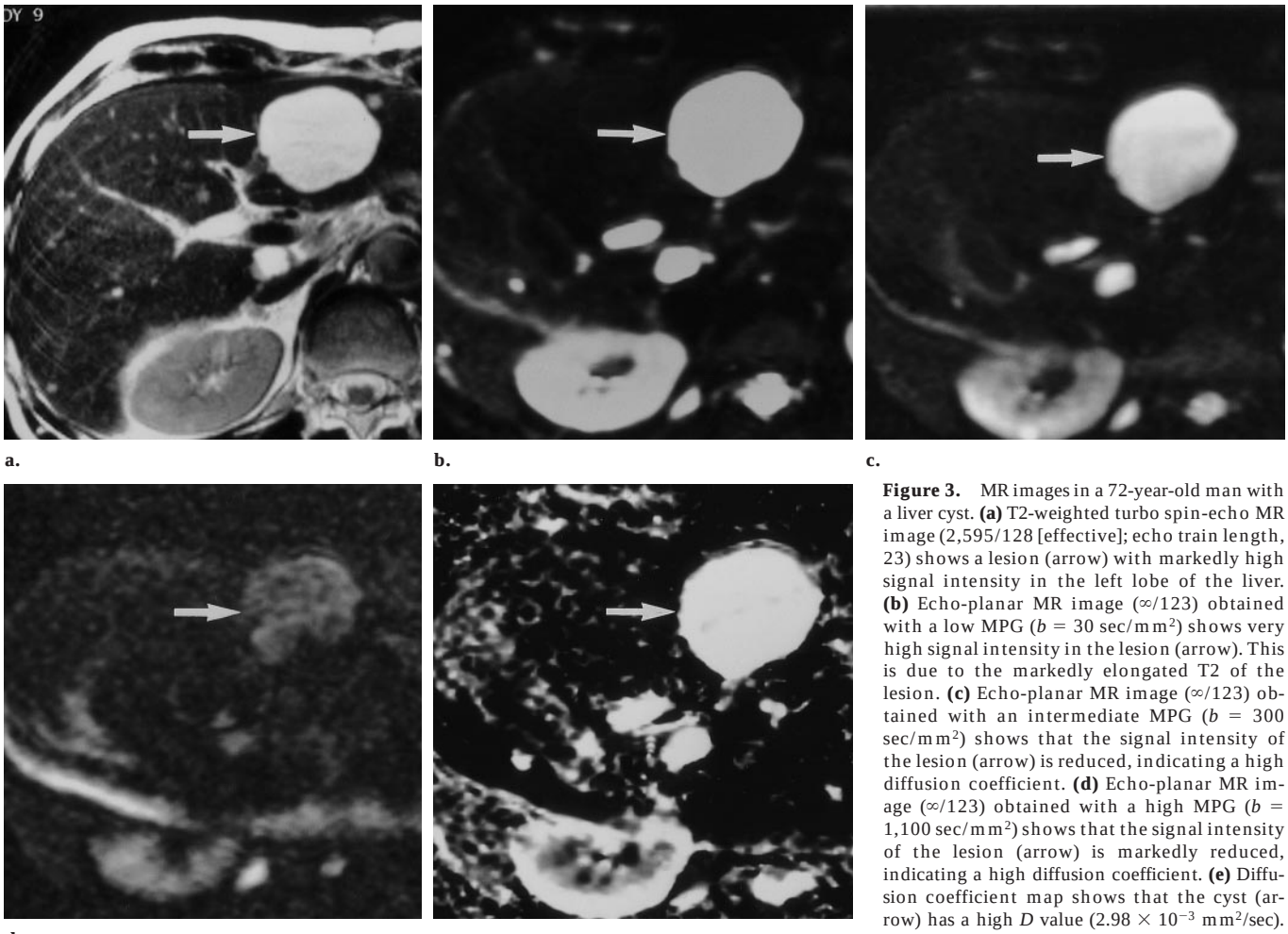

Figure 3. MR images in a 72-year-old man with a liver cyst. **(a)** T2-weighted turbo spin-echo MR image (2,595/128 [effective]; echo train length, 23) shows a lesion (arrow) with markedly high signal intensity in the left lobe of the liver. **(b)** Echo-planar MR image (∞/123) obtained with a low MPG (b = 30 sec/mm^2) shows very high signal intensity in the lesion (arrow). This is due to the markedly elongated T2 of the lesion. **(c)** Echo-planar MR image (∞/123) obtained with an intermediate MPG (b = 300 sec/mm^2) shows that the signal intensity of the lesion (arrow) is reduced, indicating a high diffusion coefficient. **(d)** Echo-planar MR image (∞/123) obtained with a high MPG (b = 1,100 sec/mm^2) shows that the signal intensity of the lesion (arrow) is markedly reduced, indicating a high diffusion coefficient. **(e)** Diffusion coefficient map shows that the cyst (arrow) has a high D value (2.98 × 10^{-3} mm^2/sec). The diffusion coefficient map was calculated on a pixel-by-pixel basis by using Equation (2).

($P < .05$) (Fig 1a). The results indicate that with diffusion-weighted IVIM MR imaging, the effect of perfusion indeed contributed to the ADC values of the solid hepatic lesions. Furthermore, the perfusion fractions of these lesions were estimated to have the following values: hepatocellular carcinomas, 0.15; metastases, 0.22; and hemangiomas, 0.35.

The ADC value of cysts was not significantly different from the D value, however, and the perfusion fraction of cysts was estimated to be 0 (Table 2, Fig 1b). These data are compatible with the fact that cysts do not have a perfusion fraction.

As shown in Table 2 and Figure 4, the D values of hepatocellular carcinomas were significantly lower than those of other hepatic lesions ($P < .05$) (Fig 2). The D values of cysts were significantly higher than those of other hepatic lesions ($P < .01$) (Fig 3). The D values of metastases were not significantly different from the those of hemangiomas. However, the perfusion fractions of metastases were significantly lower than those of hemangiomas ($P < .05$). Thus, the perfusion fractions and the D values provide useful parameters for differentiation between malignant and benign hepatic lesions.

DISCUSSION

The signal attenuation at diffusion-weighted MR imaging depends on the effects of both diffusion and perfusion (1,2). When the contribution of perfusion is not recognized, this additional cause of signal attenuation could lead to an overestimation of diffusion coefficients (3). For the gray matter of the normal human brain, a perfusion fraction of as much as 14% has been reported (3). To our knowledge, however, the effects of diffusion and perfusion in abdominal organs and hepatic lesions at diffusion-weighted or IVIM echo-planar MR imaging have not been reported.

Our data revealed that the ADC values of the liver, spleen, kidney, pancreas, and muscle were significantly higher than the diffusion coefficient D values estimated with the IVIM theory for these organs. The contribution of perfusion to the ADCs of the abdominal solid organs at diffusion-weighted MR imaging is clearly indicated in these results. However, the ADC values of the gallbladder and ascites were equal to or not significantly different from their respective D values. The ADC value of the water phantom also was equal to its D value. The findings are compatible with the fact that diffusion is the only type of motion in the gallbladder (bile), ascites fluid, and water phantom.

Furthermore, the ADC values of hepatocellular carcinomas, metastases, and hemangiomas were significantly higher than their respective D values. The results demonstrate that at diffusion-weighted MR

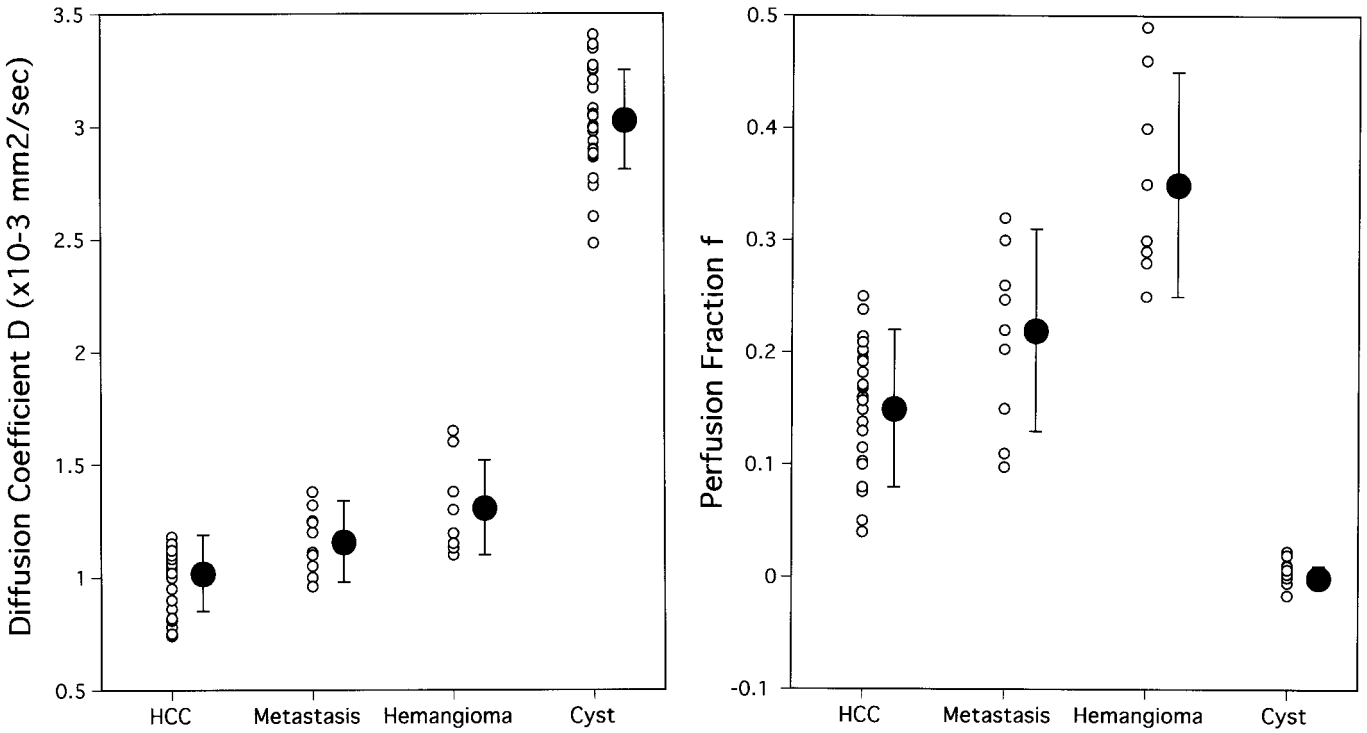

Figure 4. **(a)** Graph of diffusion coefficient *D* values (○) for the hepatic lesions in 78 patients. The *D* values for hepatocellular carcinoma (*HCC*) were significantly lower than those for other hepatic lesions ($P < .05$), and the *D* values for cysts were significantly higher than those for other hepatic lesions ($P < .01$). Error bars = SDs, ● = mean *D* value. **(b)** Graph of perfusion fraction *f* values (○) for the hepatic lesions in 78 patients. The perfusion fractions for hemangiomas were significantly higher than those for other hepatic lesions ($P < .05$). Error bars = SDs, *HCC* = hepatocellular carcinoma, ● = mean *f* value.

imaging, perfusion also contributed to the ADCs of the solid hepatic lesions. However, the ADC value and the *D* value of cysts were not significantly different, which is compatible with the fact that cysts have no perfusion fraction.

With respect to hepatic lesions, the lowest *D* values were found in hepatocellular carcinomas, and the highest *D* values were found in cysts. The *D* values of metastases were not significantly different from the *D* values of hemangiomas. However, significantly lower values of the perfusion fraction *f* were observed for metastases when compared with the values for hemangiomas, probably because the latter have a rich vascular network. The perfusion fraction *f*, in addition to the true diffusion coefficient *D*, consequently provides a useful parameter for the characterization of hepatic lesions.

When an MR signal with different values of *b* is used in Equation (2), the final part of the signal decay curve (for large values of *b*) represents diffusion almost exclusively. This is because a value of *D** that is larger than *D* can be expected, and perfusion effects are canceled out by large gradients (2,3). Thus for large values of *b*, Equation (2) is approximated by $SI/SI_o = (1 - f) \times \exp(-bD)$. In contrast to this, the first portion of the signal decay curve (for smaller values of *b*) indicates the effects of diffusion and perfusion. As a consequence, because of the perfusion, the ADC that would be calculated from low values of *b* would significantly differ from the value of *D*. With regard to this, the authors of previous reports (6,7) in which low values of *b* (1.6 and 55.0 sec/mm^2) were used noted a high value of the ADC (2.28×10^{-3} mm^2/sec) for the liver. Other investigators (4) who used low and intermediate *b* values (2–395 sec/mm^2) for the liver reported intermediate values of the ADC (1.39×10^{-3} mm^2/sec). In yet another report (5), when low (30 sec/mm^2) and high *b* values (1,200 sec/mm^2) were used, a low ADC value (0.69×10^{-3} mm^2/sec) was noted. Our results and the results noted by these other investigators therefore demonstrate that when small *b* values are used, high ADC values are obtained at diffusion-weighted MR imaging, owing to the influence of perfusion.

The ADC is an artificial parameter, without any intrinsic physical relevance, that combines diffusion and perfusion (8). The diffusion coefficient *D* as measured at IVIM MR imaging is a true parameter of molecular diffusion. It therefore permits characterization of tissues and pathologic conditions. Furthermore, the perfusion fraction *f* as measured at IVIM MR imaging provides another useful parameter with which to characterize abdominal organs and hepatic lesions. However, multiple acquisitions with different *b* values may raise some concern in noncompliant patients and with regard to other cases where time is important. In these circumstances, an ADC value calculated on the basis of intermediate and high *b* values (eg, 300 and 1,100 sec/mm^2, respectively) would probably approximate the *D* value. The latter method is probably the fastest way to assess the true diffusion coefficient *D* in abdominal organs and hepatic lesions.

In this study, we used the MPGs applied only along the section-selective direction; thus, we could not address the issue of tissue anisotropy and its effect on the calculated *D* value. Abdominal organs and hepatic lesions, however, appear to have no tissue anisotropy, with the excep-

tion of the kidney, which has substantial diffusion anisotropy (9). In addition, we did not consider the synergistic effect of the imaging gradients, that is, the cross-term contributions (10). However, the diffusion-weighted MR imaging sequence that we used demonstrated no vascular contribution for the gallbladder, ascites, water phantom, and cysts (which have no perfusion fraction). Thus, we believe that the effect of the cross terms appears to be negligible for the calculated *f* and *D* values of abdominal organs and hepatic lesions.

In conclusion, by using IVIM echo-planar MR imaging, we have demonstrated that the effect of perfusion significantly contributes to the ADCs of abdominal organs and hepatic lesions. The smaller the *b* values used, the higher the ADC values obtained at diffusion-weighted MR imaging, owing to the contribution of perfusion. The true diffusion coefficient *D* and perfusion fraction *f* are useful parameters for the characterization of hepatic lesions.

References

1. Le Bihan D, Breton E, Lallemand D, Grenier P, Cabanis E, Lavel-Jeantet M. MR imaging of intravoxel incoherent motions: application to diffusion and perfusion in neurologic disorders. Radiology 1986; 161:401–407.
2. Le Bihan D, Breton E, Lallemand D, Aubin ML, Vignaud J, Lavel-Jeantet M. Separation of diffusion and perfusion in intravoxel incoherent motion MR imaging. Radiology 1988; 168:497–505.
3. Turner RT, Le Bihan D, Maier J, Vavrek R, Hedges LK, Pekar J. Echo-planar imaging of intravoxel incoherent motion. Radiology 1991; 177:407–414.
4. Müller MF, Prasad P, Siewert B, Nissenbaum MA, Raptopoulos V, Edelman RR. Abdominal diffusion mapping with use of a whole-body echo-planar system. Radiology 1994; 190:475–478.
5. Namimoto T, Yamashita Y, Sumi S, Tang Y, Takahashi M. Focal liver masses: characterization with diffusion-weighted echo-planar MR imaging. Radiology 1997; 204: 739–744.
6. Ichikawa T, Haradome H, Hachiya J, Nitadori T, Araki T. Diffusion-weighted MR imaging with single-shot echo-planar imaging in the upper abdomen: preliminary clinical experience in 61 patients (abstr). In: Proceedings of the Fifth Meeting of the International Society for Magnetic Resonance in Medicine. Berkeley, Calif: International Society for Magnetic Resonance in Medicine, 1997; 936.
7. Ichikawa T, Haradome H, Hachiya J, Nitatori T, Araki T. Diffusion-weighted MR imaging with a single-shot echoplanar sequence: detection and characterization of focal hepatic lesions. AJR 1998; 170: 397–402.
8. Le Bihan D. Intravoxel incoherent motion imaging. In: Le Bihan D, ed. Diffusion and perfusion magnetic resonance imaging: applications to functional MRI. New York, NY: Raven, 1995; 270–274.
9. Mueller MF, Prasad PV, Bimmler D, Kaiser A, Edelman RR. Functional imaging of the kidney by means of measurement of the apparent diffusion coefficient. Radiology 1994; 193:711–715.
10. Neeman M, Freyer JP, Sillerud LO. Effects of imaging gradients on diffusion measurements by MR imaging. In: Le Bihan D, ed. Diffusion and perfusion magnetic resonance imaging: applications to functional MRI. New York, NY: Raven, 1995; 73–76.